

Supplementary Material: Atomically dispersed Ni single-atoms anchored on N-doped graphene aerogels for highly efficient electromagnetic wave absorption

Bing Suo, Xiao Zhang*, Xinyu Jiang, Feng Yan*, Zhengzhi Luo, Yujin Chen*

Key Laboratory of In-Fiber Integrated Optics, Ministry of Education and College of Physics and Optoelectronic Engineering, Harbin Engineering University, Harbin 150001, China. E-mail address: chenyujin@hrbeu.edu.cn.

EXPERIMENTAL SECTION

Materials. Graphene oxide (GO) was purchased from Shenzhen Yuechuang Evolution Technology Co., Ltd., nickel chloride hexahydrate ($\text{NiCl}_2 \cdot 6\text{H}_2\text{O}$), dicyandiamide (DCD), and ethanol ($\text{C}_2\text{H}_5\text{OH}$) were purchased from Tianjin Guangfu Fine Chemical Research Institute (China). All chemicals were used directly without further purification.

Synthesis of NRGA. Graphene oxide (GO) (50 mg) was dispersed in water (10 mL) under the sonication for 30 min. Then the suspension was transferred into a Teflon-lined stainless-steel autoclave, and hydrothermally treated at 180 °C for 10 hours. The prepared hydrogel was freeze-dried for 24 hours. The obtained aerogel was immersed in the 25 mL of ethanol containing 0.35 g of dicyandiamide, and then hydrothermally treated at 180 °C for 2 hours. Finally, the GA was heated at 900 °C for 2 hours under argon atmosphere to obtain NRGA.

Synthesis of Ni-NP@NRGA. GO (50 mg) was dispersed in water (10 mL) under the sonication for approximately 30 min. Then the suspension was transferred into a Teflon-lined stainless-steel autoclave, and hydrothermally treated at 180 °C for 10 hours. The prepared hydrogel was freeze-dried for 24 hours. The obtained aerogel was immersed in 50 mL ethanol/water (v:v = 1:1) containing 0.7 g of nickel chloride hexahydrate and 0.35 g of dicyandiamide, and then hydrothermally treated at 180 °C for 2 hours. Finally, the GA was heated at 900 °C for 2 hours under flowing argon to

obtain Ni-NP@NRGA.

Synthesis of Ni-SA@NRGA. The obtained Ni-NP@NRGA was treated 2 M H₂SO₄ solution at 80°C for 12 h to remove the Ni nanoparticles.

Characterizations. The morphology, size and structure of all samples was observed using a Hitachi SU8000 scanning electron microscope (SEM) at an accelerating voltage of 15 kV and the test current of 10 μA. The sample was mixed with ethanol under ultrasonic to uniform dispersion, after that drop dispersion solution onto the copper sheet which fixed with conductive tape, then placed into the cavity mirror for observation. The refined structure, crystallization, morphology, particle size and composition of the material were characterized by Hitachi JEM-2100 transmission electron microscope operating at a voltage of 200 kV. The sample was mixed with ethanol by ultrasonic until it was evenly dispersed before the test, and then dropped dispersion solution onto the micro-grid and observed under the endoscope. The crystal structure and composition of the synthesized samples were characterized by X-ray powder diffraction (XRD) using a X Pert Pro diffractometer with Cu Kα radiation ($\lambda=1.5418 \text{ \AA}$) in the scattering range (2θ) of 15–90° with a scanning rate of 5°/min. The surface chemical compositions and valence states were qualitative analyzed by X-ray photoelectron spectroscopy (XPS, K-Alpha, ThermoFisher Scientific Company). Raman spectra was used to characterize the disorder degree of carbon materials and acquired at room temperature by Lab RAM Aramis micro Raman spectrometer in the range of 500–2500 cm⁻¹ with an excitation wavelength at 488 nm. The magnetic properties of samples were measured using a vibrating sample magnetometer (VSM; Lakeshore 7404) at room temperature. Metallic elemental content of the samples was analyzed by inductively coupled plasma-optical emission spectroscopy (ICP-OES) were tested by iCPA 7000 Series spectrometer.

Electromagnetic parameter measurement. The microwave absorption properties and electromagnetic parameters of the absorbing materials were measured by using a vector network analyzer (Anritsu MS4644A Vectorstar) in the range of 2–18 GHz at the room temperature. The absorbing materials (25 wt%) to be tested is mixed with paraffin wax, and a specific abrasive tool is used to form a ring (ring inner diameter

3.04 mm, outer diameter 7.0 mm, thickness about 2.5 mm), and then the electromagnetic parameters of the sample are measured by the coaxial transmission/reflection method.

The reflection loss is used to evaluate the electromagnetic wave absorption ability of the material through the reflection loss R_L (Reflection loss) (dB) of the material to the electromagnetic wave. According to transmission line theory, the formula for reflection loss is as follows:

$$Z_{in} = Z_0 \sqrt{\frac{\mu_r}{\epsilon_r}} \tanh \left(j \frac{2\pi f d \sqrt{\mu_r \epsilon_r}}{c} \right) \quad (S1)$$

$$R_L(dB) = 20 \log_{10} \left| \frac{Z_{in} - Z_0}{Z_{in} + Z_0} \right| \quad (S2)$$

Among them, Z_{in} , Z_0 , ϵ_r , μ_r are the input impedance of the absorbing material, the inherent impedance of air, the relative complex permittivity and the permeability, respectively; where c, f, and d are the speed of light, electromagnetic wave frequency and coating layer thickness, respectively.^[1]

The impedance matching characteristic can be estimated the extent of impedance matching, where $|Z|$ is the normalized impedance^[2], its expression is as follows:

$$|Z| = |Z_{in}| / |Z_0| \quad (S3)$$

For the attenuation condition, in order to make the attenuation ability of materials to electromagnetic waves better, the material often needs to have a large attenuation coefficient α , which is often used to measure the attenuation ability of materials to electromagnetic waves, its expression is as follows:

$$\alpha = \frac{\sqrt{2\pi f}}{c} \sqrt{(\mu''\epsilon'' - \mu'\epsilon')^2 + (\mu''\epsilon'' - \mu'\epsilon')^2 + (\mu'\epsilon'' + \mu''\epsilon')^2} \quad (S4)$$

In formula (S3), ϵ' and ϵ'' represent the real and imaginary parts of the material's complex permittivity, respectively; μ' and μ'' respectively represent the real and imaginary parts of the complex permeability.^[3]

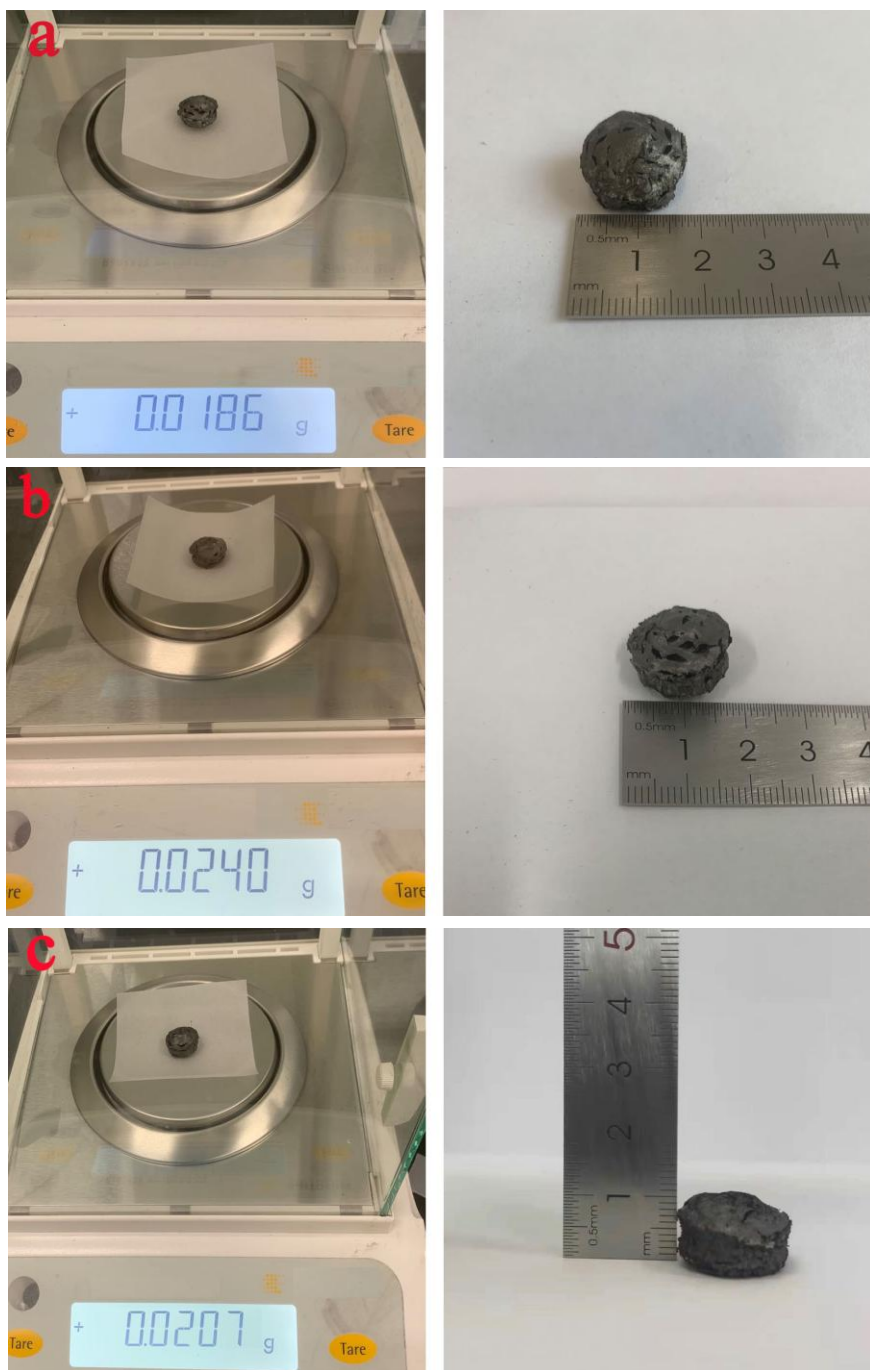


FIG. S1:The digital photographs of (a) NRGA , (b) Ni-NP@NRGA and (c) Ni-SA@NRGA.

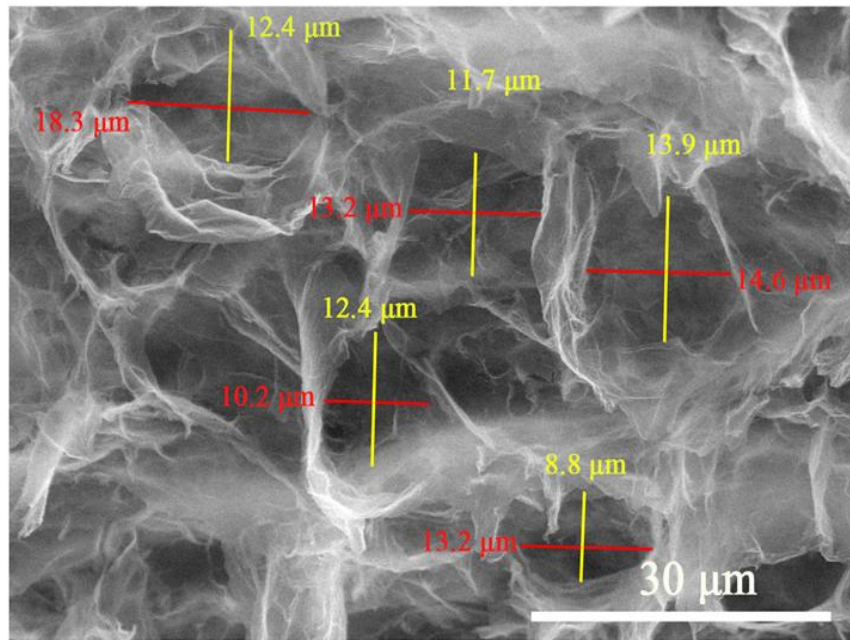


FIG. S2: SEM image of Ni-SA@NRGA.

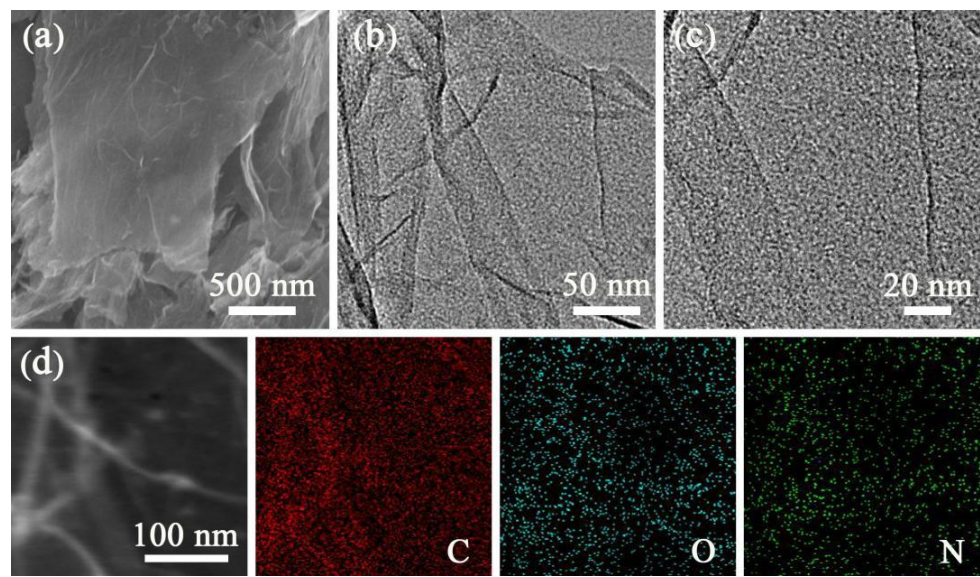


FIG. S3: (a) SEM image of NRGA. (b) TEM images of the NRGA. (c) HRTEM images of the NRGA. (d) TEM image and the corresponding EDX C, N and O mappings of NRGA.

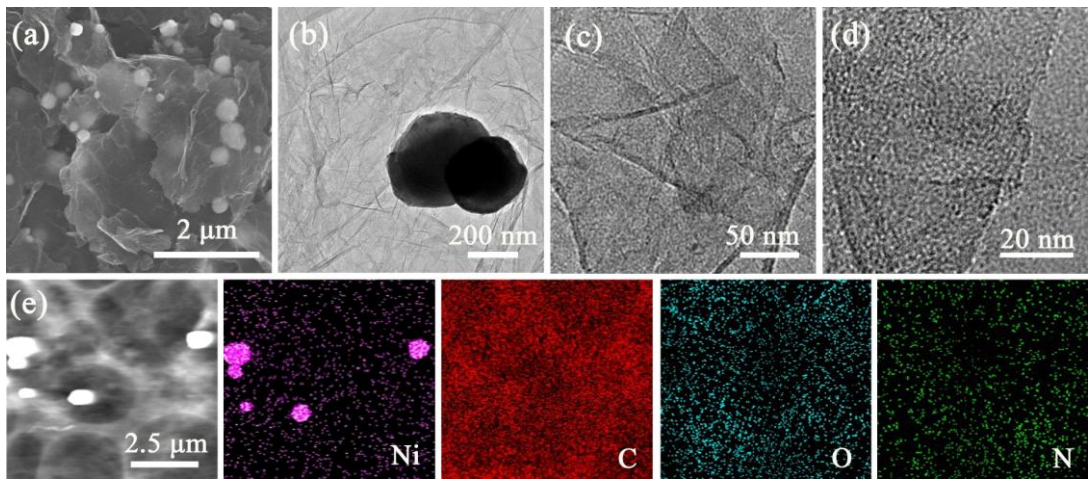


FIG. S4: (a) SEM images of the Ni-NP@NRGA. (b) TEM images of the Ni-NP@NRGA. (c) HRTEM images of the Ni-NP@NRGA. (d) TEM image and the corresponding EDX Ni, C, N and O mappings of Ni-NP@NRGA.

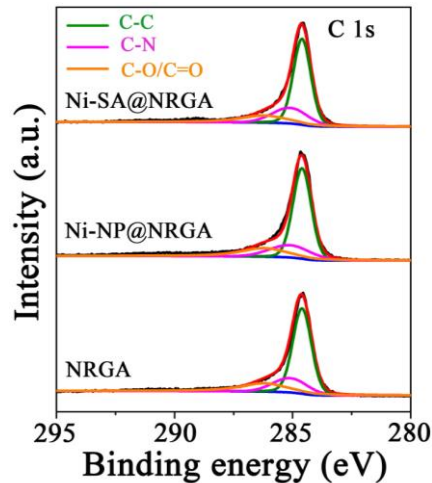


FIG. S5: XPS spectra of C 1s of Ni-SA@NRGA , Ni-NP@NRGA and NRGA.

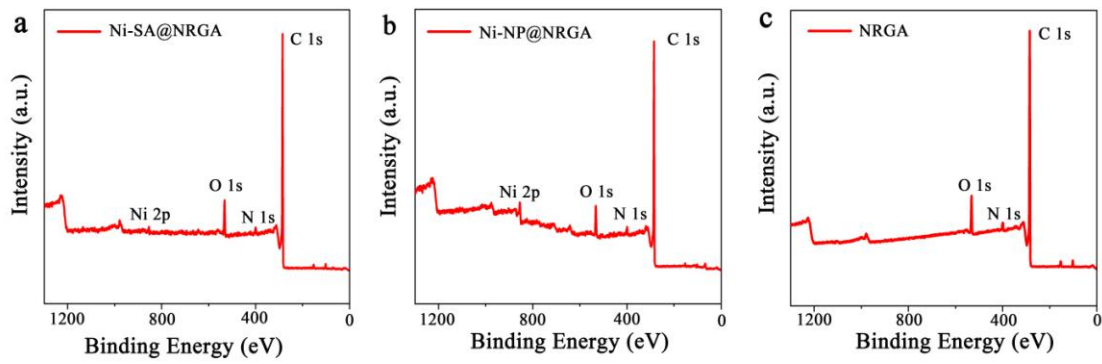


FIG. S6: XPS survey spectra of the (a) Ni-SA@NRGA, (b) Ni-NP@NRGA and (c) NRGA.

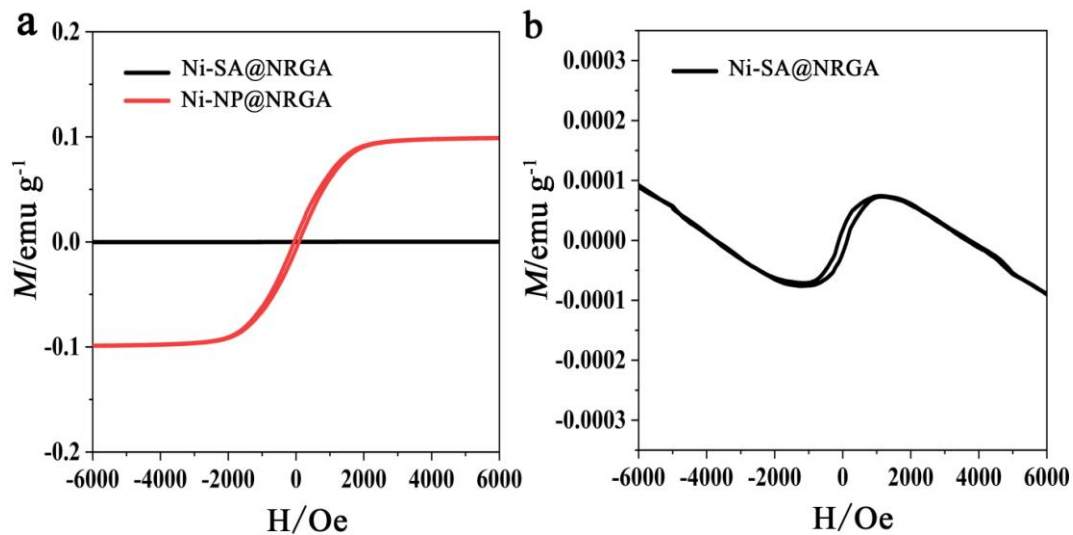


FIG. S7: The magnetic hysteresis loops of the (a) Ni-SA@NRGA and Ni-NP@NRGA, (b) an enlarged image of the Ni-SA@NRGA

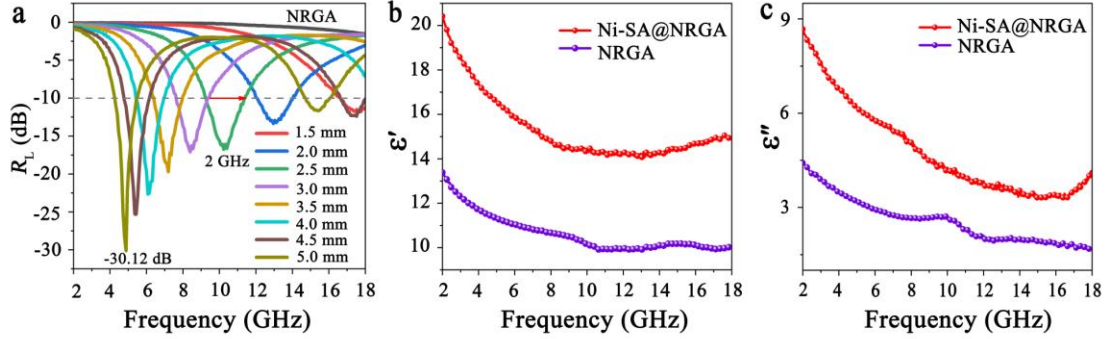


FIG. S8: (a) The reflection loss (R_L) of NRGA at d in range of 1.5mm-5.0mm. (b)-(c)The real part (ϵ') , the imaginary part (ϵ'') value of the complex permittivity of the Ni-SA@NRGA and NRGA.

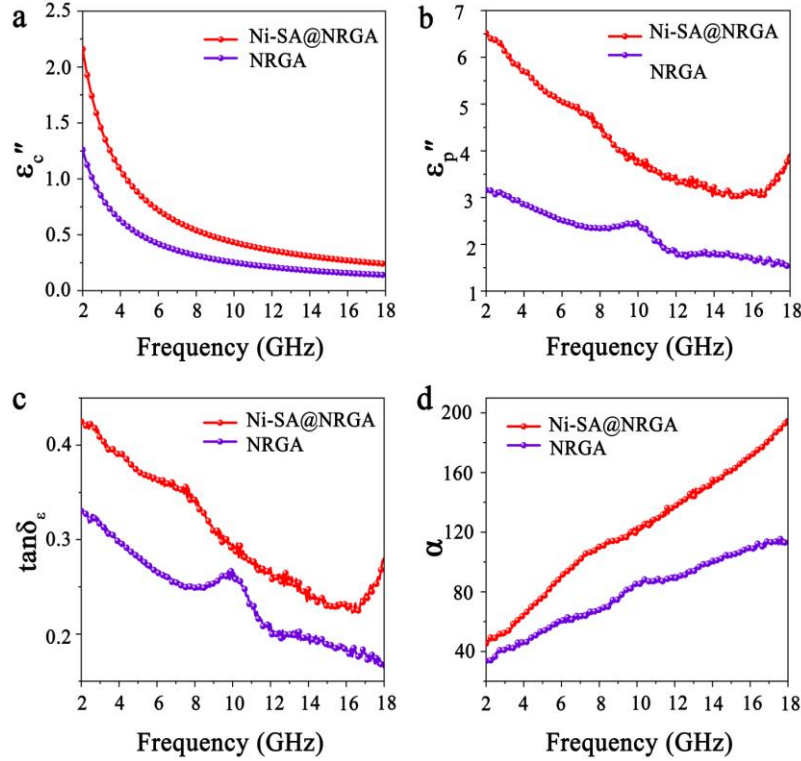


FIG. S9: (a) Conductive loss and (b) polarization loss of Ni-SA@NRGA and NRGA. (c) The dielectric loss tangents of the Ni-SA@NRGA and NRGA. (d) The attenuation coefficient α of Ni-SA@NRGA and NRGA.

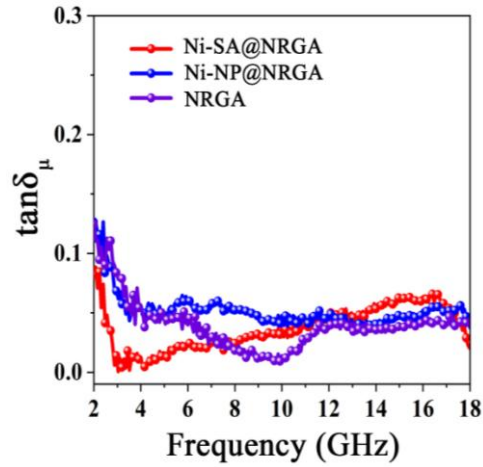


FIG. S10: The magnetic loss tangent of the Ni-SA@NRGA, Ni-NP@NRGA and NRGA.

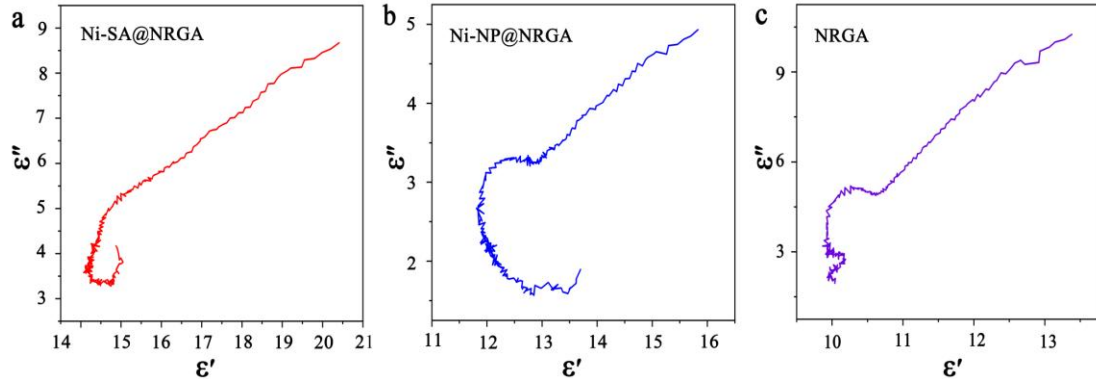


FIG. S11: ϵ' - ϵ'' plots of (a) Ni-SA@NRGA, (b) Ni-NP@NRGA and (c) NRGA.

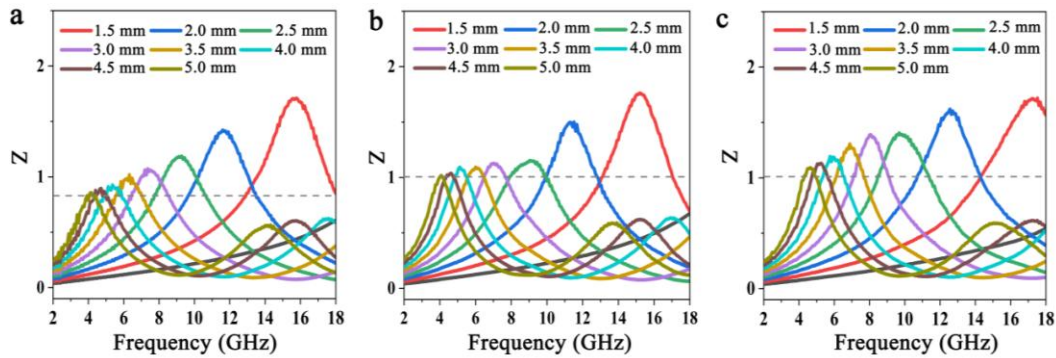


FIG. S12: The impedance coefficient $|Z|$ of the (a) Ni-SA@NRGA, (b) Ni-NP@NRGA and (c) NRGA.

Table S1. EMW Absorption Properties of 3D Ni-SA@NRGA and Other Reported Carbon-based Absorbers

Absorbers	R _{Lmin} (dB)	Thickness (mm)	Filler Ratio (wt%)	Ref.
GO/CNT-Fe ₃ O ₄	-28.57	2.00	30	4
Graphene/Fe ₃ O ₄ /Ni composites	-16.38	3.50	60	5
CF-RGO-Ni	-34.09	3.00	30	6
Core-shell Ni@graphene	-31.42	4.25	30	7
NiO/CNTs composites	-25.40	2.00	20	8
MWCNTs/ferrite composites	-18.17	5.00	40	9
<i>h</i> -Ni(245)/GN nanocomposites	-17.80	5.00	60	10
ZnFe ₂ O ₄ @ZnO@rGO nanocomposites	-35.20	2.00	30	11
n-FeNi ₃ /GN nanocomposites	-29.00	5.00	60	12
Ti ₃ C ₂ Tx@RGO composite aerogel	-31.20	3.05	15	13
Fe ₃ O ₄ /RGO	-22.70	3.00	30	14
Ni _{0.5} Co _{0.5} Fe ₂ O ₄ /graphene	-30.92	4.00	50	15
CoFe ₂ O ₄ rugbies/graphene composites	-39.00	2.00	60	16
C@NiCo ₂ O ₄ @Fe ₃ O ₄	-43.00	3.40	60	17
RGO/ZnO hollow spheres	-45.05	2.20	50	18
N-SA/Ni-6%	-42.20	2.00	50	19
Ni-SA@NRGA	-49.46	2.00	25	This Work

References

- [1] Yan J, Huang Y, Liu X D, Zhao X X, Li T H, Zhao Y and Liu P B 2021 *Polym. Rev.* **61** 646
- [2] Zhang X, Xu J, Liu X Y, Zhang S, Yuan H R, Zhu C L, Zhang X T and Chen Y J 2019 *Carbon* **155** 233
- [3] Wang K F, Chen Y J, Li H, Chen B B, Zeng K, Chen Y L, Chen H C, Liu Q L and Liu H Z 2019 *ACS Appl. Nano Mater.* **2** 8063
- [4] Yan S J, Wang L N, Wang T H, Zhang L Q, Li Y F and Dai S L 2016 *Appl. Phys. A* **122** 235
- [5] Huang Y W, Wang Y J, Wei S C, Liang Y, Huang W, Wang B and Xu B S 2019 *Int. J. Mod. Phys. B* **33** 1940055
- [6] Li J, Bi S, Mei B, Shi F, Cheng W L, Su X J, Hou G L and Wang J J 2017 *J. Alloys Comp.* **717** 205
- [7] Liu Y, Zhang X Y, Chen X, Wu Y X, Zhang C L, Wang J, Ji J Land Li K X 2021 *J. Mater. Chem. C* **9** 4910
- [8] Wang J, Jia X L, Wang T H, Geng S, Zhou C, Yang F, Tian X J, Zhang L Q, Yang H T and Li Y F 2016 *J. Alloys Comp.* **689** 366
- [9] Sun Z G, Qiao X J, Wan X, Ren Q G, Li W C, Zhang S Z and Guo X D 2016 *Appl. Phys. A* **122** 87
- [10] Chen T T, Deng F, Zhu J, Chen C F, Sun G B, Ma S L and Yang X J 2012 *J. Mater. Chem.* **22** 15190
- [11] Li F, Zhuang L, Zhan W W, Zhou M X, Sui G, Zhou A S, Bai G, Xiao W, Yang X P 2020 *Ceram. Int.* **46** 21744
- [12] Ma T, Yuan M W, Islam S M, Li H F, Ma S L, Sun G B and Yang X J 2016 *J. Alloys Compd.* **678** 468
- [13] Wang L B, Liu H, Lv X L, Cui G Z and Gu G X 2020 *J. Alloys Compd.* **828** 154251
- [14] Wu J M, Ye Z M, Liu W X, Liu Z F and Chen J 2017 *Ceram. Int.* **43** 13146
- [15] Yin P F, Deng Y, Zhang L M, Wu W J, Wang J, Feng X, Sun X Y, Li H Y and Tao Y 2018 *Ceram. Int.* **44** 20896
- [16] Zhang S L, Jiao Q Z, Hua J, Li J J, Zhao Y, Li H S and Wu Q 2015 *J. Alloys Comp.* **630** 195
- [17] Wei S A, Wang X X, Zhang B Q, Yu M X, Zheng Y W, Wang Y and Liu J Q 2017 *Chem. Eng. J.* **314** 477
- [18] Han M K, Yin X W, Kong L, Li M, Duan W Y, Zhang L T and Cheng L F 2014 *J. Mater. Chem. A* **2** 16403
- [19] Gao S S, An Q D, Xiao Z Y, Zhai S R and Yang D J 2018 *ACS Appl. Nano Mater.* **1** 5895